Project funded by the European Commission under the 6th (EC) RTD Framework Programme (2002- 2006) within the framework of the specific research and technological development programme “Integrating and strengthening the European Research Area”

Project UpWind

Contract No.:
019945 (SES6)

“Integrated Wind Turbine Design”

Wp8: Flow

Deliverable D8.1 Data

Wake measurements used in the model evaluation

AUTHOR:	Kurt S. Hansen
AFFILIATION:	Department of Mechanical Engineering, Technical University of Denmark
ADDRESS:	Nils Koppels Allé, B403-DTU, DK-2800 Lyngby
TEL.:	+45 4525 4318
EMAIL:	ksh@mek.dtu.dk
FURTHER AUTHORS:	R. Barthelmie University of Edingburgh/Risø National Laboratory D. Cabezon CENER E. Politis CRES
REVIEWER:	WP8 Project members
APPROVER:	

Document Information

DOCUMENT TYPE	Deliverable D8.1
DOCUMENT NAME:	WP8Flow8.1D1.doc
REVISION:	
REV.DATE:	18 June 2008
CLASSIFICATION:	PU
STATUS:	Final

Abstract: Three wind farm flow cases with turbine different spacing have been defined for validating the wake deficit calculations inside an offshore wind farm. The measured wake deficit is determined for a number of flow directions in the 160MW Horns Rev wind farm.

Contents

STATUS, CONFIDENTIALITY AND ACCESSIBILITY									
Status				**Confidentiality**				**Accessibility**	
S0	Approved/Released	**x**		**R0**	General public	**x**		Private web site	
S1	Reviewed			**R1**	Restricted to project members			Public web site	
S2	Pending for review			**R2**	Restricted to European. Commission			Paper copy	
S3	Draft for commends			**R3**	Restricted to WP members + PL				
S4	Under preparation			**R4**	Restricted to Task members +WPL+PL				

PL: *Project leader* **WPL:** *Work package leader* **TL:** *Task leader*

1. Introduction

It is evident that wake or wind farm models have not been evaluated for very large wind farms. Since the combination of single wakes is the current approach to modeling wakes within offshore wind farms, there is major uncertainty in these predictions of wake interactions. For very large wind farms single wake or local momentum balance approaches may be insufficient, since the wind farm must be expected to interact with the wind climate, giving rise to a complicated flow pattern. One way of viewing/simplifying the problem is that on the larger scale the wind farm adds to the terrain surface roughness and thus resulting in a wind speed reduction on top of the reduction stemming from the individual wakes. i.e. determining the extent of the macro-scale effect. Presently, no solid empirical information is available to assess accuracy of the industry standards in software for GW-size wind farms. However, it is known that ignoring the large-scale effect (interaction with the boundary-layer) will result in optimistic estimates of the necessary separation distance for large wind farms. Present engineering codes suggest that 1-2km of separation will allow the flow to regenerate whereas roughness change models indicate that an order of magnitude larger separation is needed for the wind speed to recover.
This document defines test cases from both complex terrain and offshore, which can be identified from existing wind farm measurements, and used for validation of modeled wakes within large wind farms.

1.1 Types of measurements

There are essentially two types of measurements; meteorological and wind farm data. Some wind farms retain the meteorological mast(s) that was/were established for the resource determination and if these data are available in addition to wind farm data it is an added bonus particularly with regard to questions such as ‘What is the wind farm power curve?’ (depending on the mast location). At few offshore wind farms such as Vindeby, Bockstigen, Horns Rev and Nysted one or more meteorological masts were added after construction to aid research.

Meteorological data can also be divided into two types – mast and remotely sensed data. Examples of wind farms supported by meteorological mast data include Nørrkær Enge, Vindeby, Horns Rev and Nysted. The advantage of meteorological mast data is that it is usually available for a long period, it is typically accurate (although this can depend on the mast structure) and wind speed, direction and turbulence profiles to hub-height are usually available at a good time resolution and with high data capture. The most obvious disadvantage is that the location of the measurements is fixed so from a wake perspective the wake distance is fixed. However, wake analysis has to be made for specific directional sectors and the wake distances can vary according to the layout of the wind farm and the position of the mast. Measurements are rarely made above hub-height.

Remote sensing is providing additional types of information for use in wind energy. We exclude here satellite data although these have been used both for wind resource and for wakes estimation. Both sodar and doppler lidar are able to measure wind speed profiles both beyond and above hub-height and may be particularly useful offshore due to the expense of erecting tall meteorological masts in this environment. Data from both instruments requires additional processing and maybe subject to some accuracy or operational limitations but progress has been made to the point where Doppler lidar in particular may become a standard instrument. As yet, there have been limited studies using sodar or lidar in wake studies. Obviously for wake studies in large wind farms, wind farm data are needed. Parameters required would typically be the power output, nacelle direction and yaw misalignment and additional operational information such as a status signal. These data are routinely collected using Supervisory Control And Data Acquisition (SCADA) systems although storage and retrieval of these data for research purposes may be a time consuming process. A more significant issue is that all wind farm data are typically confidential and developers are reticent to share raw data. This is a big issue in

model evaluation exercises where data are necessary and also by the nature of the exercise many different groups are involved. Nevertheless it is clear that access to data is critical at this point while the wind farm model evaluation for more challenging environments is conducted.

1.2 Issues comparing models and measurements

There are some major issues in wind farm model validation studies which will be discussed below. As stated above we concentrate here on power loss modelling which should encompass the whole range of wind speeds and directions and we also consider that the range of wind farm/wake model extends from engineering through to full CFD models. In general, computing requirements for CFD models means we are restricted to examining a number of specific wind speed and direction cases and only a moderate number of turbines rather than wind farms with ~100 turbines which can easily be done by WindFarmer and WAsP. On the other hand it can be difficult to extract reasonable simulations from some of the wind farm models for very specific cases. For example, WAsP relies on having a Weibull fit to wind speed distributions and fairly large directional sectors (30°). Therefore for specific wind speeds and narrow directional bins models like WAsP are never going to produce very exact solutions because they are being used beyond their operational windows. In addition to this there are a number of specific issues:

- Establishing the freestream flow. The major issues in determining the freestream flow are the displacement of the measurement mast from the array (assuming there is a mast), adjustments in the flow over this distance especially in coastal areas and differences in height between the measurement and the turbine hub-height. If there is no mast or the mast is in the wake of turbines or subject to coastal flow then the turbine(s) in the freestream flow may be used. If power measurements are used to determine wind speed they will be subject to any errors in the site specific power curve.
- Wind direction, nacelle direction and yaw misalignment. Because of the difficulty in establishing true north when erecting wind vanes (especially offshore where landmarks may not be determinable) it can be difficult to establish a true freestream direction. Even a well maintained wind vane may have a bias of up to 5° and it is important to understand this because the total width of a wake may be of the order 10-15° at typical turbine spacing. In a large wind farm, each turbine may have a separate bias on the direction, which is very difficult to determine. Analysis must be undertaken to calibrate the maximum wake direction to within 1° and to check for bias of the yaw angle on each wind turbine in the array.
- If there is a gradient of wind speeds across the wind farm as there may be e.g. in coastal areas, near a forest or caused by topography these variations will need to be accounted for before wake calculations are undertaken.
- In terms of modelling wakes both the power curve and thrust coefficients must be known but these will vary according to the specific environment. A power curve must be calculated for the site. For modelling, the question of whether the thrust coefficient should be set to one value for the wind farm or at each individual turbine in each simulation is still an open one. The state-of-the-art is to validate the individual power and pitch curves with reference to the nacelle anemometer, which seems to be a rather robust method to determine changes in the system setup.
- Comparing the modelled standard deviation of power losses in a row with the measured standard deviation raises a number of issues. The two most important are ensuring that the time averaging is equivalent between models and measurements and taking into account that there will be natural fluctuations in the wind speed and direction in any period. Models are typically run for specific directions but it may be necessary to include the standard deviation of the wind direction in the model simulations.
- In the large wind farm context the time scale of wake transport must be considered. A large wind farm with 100 turbines in a 10 by 10 array with an 80 m diameter rotor and a space of 7 rotor diameters has a length of nearly 6 km. At a wind speed of 8 m/s the travel time through the array is more than 10 minutes. As mentioned above the wind

direction will be subject to natural fluctuations in addition to possible wake deflection but there will also be natural variations in the wind speed over this time scale.

- Determining turbulence intensity and stability may be critical. Turbulence intensity is a key parameter in many models. Using either mast data to determine this information or deriving it from turbine data is subject to fairly large errors for the reasons discussed above and because the accuracy of temperature measurements used to derive stability parameters is often inadequate.

2. Offshore cases: Horns Rev Wind farm measurements

2.1 Definition of offshore wind farm flow cases

Due to an agreement with DONG Energy A/S (formerly ELSAM Engineering A/S) it has been possible to obtain access to one year of offshore recordings from the Horns Rev wind farm recorded during 2005. The dataset from Horns Rev offshore wind farm includes 10-minute mean values of power, nacelle position, pitch angle and yaw misalignment from each wind turbine together with wind speeds and wind directions on the near by three metrological mast. The data set represents a full operational year with very high park availability.
During the WP8 kick-off meeting is was decided to define three basic flow cases according to the discussions listed in the minutes [2].
The flow cases represent three different wind turbine spacing, which are a fundamental parameter when validating the wake deficit. The spacing, which is determined by the wind farm layout, cannot be changed, is defining three basic flow cases with uniform inflow representing a long velocity fetch distance:

Case	Spacing	Wind direction	V_{hub}
1:	7.0×D	270 deg.	6 ± 0.5, 8 ± 0.5 & 10 ± 0.5 m/s
2:	9.4×D	221 deg.	6 ± 0.5, 8 ± 0.5 & 10 ± 0.5 m/s
3:	10.4×D	312 deg.	6 ± 0.5, 8 ± 0.5 & 10 ± 0.5 m/s

The downwind power deficit and the derived speed deficit are determined for each flow case during different flow conditions e.g. atmospheric stability classes, wind directional sectors and wind speed bins in the following chapter.

2.2 Park layout

Horns Rev Wind Farm consists of an 8 row (east to west) by 10 column (north to south) matrix of 80 turbines. The vertical columns are aligned approximately 7.2° West of North - forming a parallelogram. The spacing between turbines in both the rows and columns is 7D (=560m). The spacing between turbines in the south-west to north-east diagonal (221°) is 9.4D (appr.750m) and in the north-west diagonal (312°) is 10.4D (appr.840m) as indicated on Figure 1. Further information about the park layout is given in [1] and the location of the three meteorological masts outside the park is shown in Appendix A.

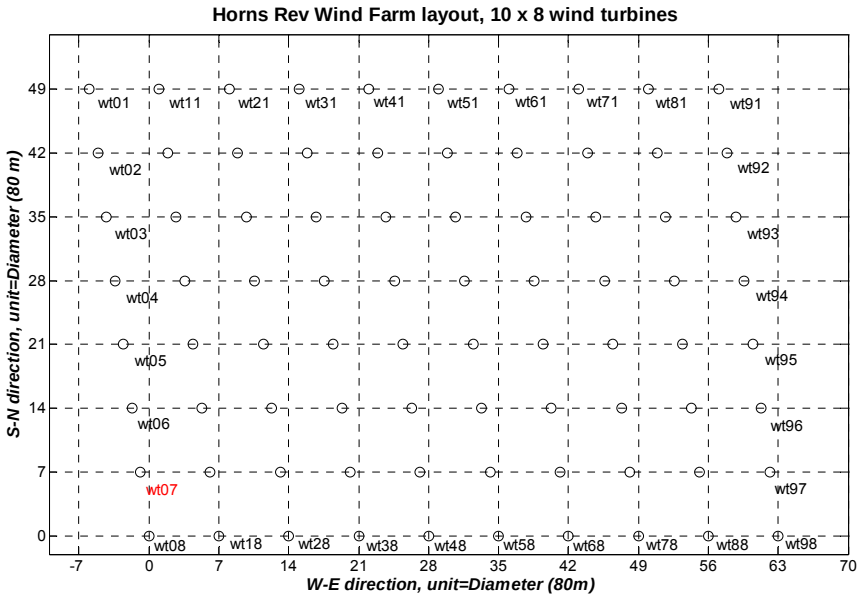

Figure 1: Layout of Horns Rev Wind Farm, where the reference wind turbine (wt07) is located in the SW corner of the park.

2.3 Data screening

The Horns Rev data set contains a number of representative 10-minute statistical values from each wind turbine e.g. electrical power, pitch angle, wind speed and direction measured on nacelle, nacelle position and the turbine run counter.
All the measurements have been validated according to a proper power signal level compared to nacelle wind speed and mean pitch angle. Furthermore all events like idling, start and stop sequences and reduced power levels have been marked with a index, which has been included the selection of measurements for the flow cases.

The meteorological properties have been recorded and stored as 10 minute mean values from 3 masts near the wind turbines as indicated in [3] and Appendix A. All measurements are checked during inter-comparison and outliners have been marked with a (quality) index.

2.3.1 Atmospheric stability.

The atmospheric stability at Horns Rev during 2005 is based on the difference between water and air temperatures at the wake mast M7 located between park and land due to good signal availability. The Richardson number (*Ri*) is calculated according to (1)

$$Ri = 9.81/(273.15+T_u)\times((T_u-T_l)/\Delta h_T)/\,sqr((V_{70}-V_{20})/\Delta h_V) \qquad (1)$$

Sensor	Air/water	Air/air
T_u - degC	h = 64 m (asl)	h = 64 m
T_l - degC	h = -3 m (bsl)	h = 64 m
V_{70}	h = 70 m	h = 70 m
V_{16}	h = 20 m	h = 20 m
z'	31 m	37.5 m

Note the wake situations with reduced wind speed at hub height have not been eliminated. The atmospheric stability (z/L) with a reference height z' is defined according to:

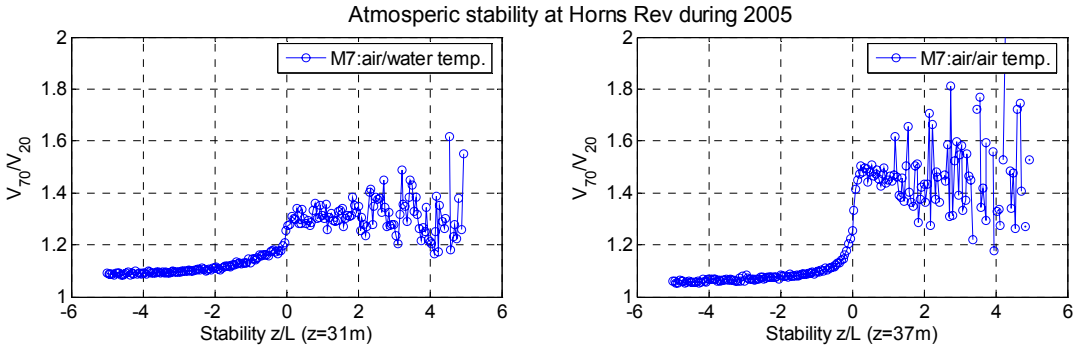

Figure 2: Distribution of atmospheric stability measured at Horns Rev during 2005; a) air/water difference and b) air/air temperature difference.

The available periods covers 8.606 hours during 2005, as shown on Figure 2, are classified in stability classes as listed in Table 1. The main part of wind farm measurements used the analysis have been recorded during (slightly) unstable atmospheric stratification (-12 <z'/L <-2) with reference to air/air stability.

Table 1: Stability classes for Horns Rev measurements during 2005, based on air/air temperature measurements.

Very unstable; z/L < -12	**1920 hours**
Unstable, -12< z/L<-2	**1881 hours**
Near neutral, -2 < z/L < +2	**2618 hours**
Stable; z/L> 2	**2187 hours**
Total	**8606 hours**

While all temperatures from Horns rev are recorded with absolute thermometers and undocumented calibration and low resolution, the resolution of the temperature difference is low. All analysis performed on the Horns Rev measurements in the following chapters are based on the air/air stability.

2.3.2 Power curves

The electrical power curve has been determined for 5 turbines, during unstable conditions and in two distinct, free sectors. The main purpose of validating the power curves for a number of turbines with free undisturbed inflow is to determine a reference power curve. The reference power curve is based on the curves for wind turbine wt01, wt07, wt09, wt95 and wt98 respectively.

1) Eletrical power from wind turbine wt01, wt05 & wt07 combined with wind speed from mast M2, 67 m, from a 45 degree western sector.
2) Eletrical power from wind turbine wt95 & wt97 combined with the wind speed from mast M7, 70 m, from a 45 degree eastern sector.

The variation between the power curves on Figure 3 is small and this result in a robust derived [mean] curve, especially in the area of interest between 5.5 – 10.5 m/s. The reference power curve values (below rated power) are listed in Table 3 and reflect operation with a pitch angle of approximately -1°.

The reference power curve is assumed to be representative for each of the 80 wind turbines in the wind farm.

Table 2: V80 power and thrust curves from [3].

wind speed	power,kW	thrust coeff.
4	66.6	0.818
5	154	0.806
6	282	0.804
7	460	0.805
8	696	0.806
9	996	0.807
10	1341	0.793
11	1661	0.739
12	1866	0.709
13	1958	0.409
14	1988	0.314
15	1997	0.249
16	1999	0.202
17	2000	0.167
18	2000	0.140
19	2000	0.119
20	2000	0.102
21	2000	0.088
22	2000	0.077
23	2000	0.067
24	2000	0.060
25	2000	0.053

Please note that the power and thrust coefficient curves listed in Table 2 are specific to the turbines delivered for the Horns Rev Wind farm and may not apply to V80 turbines delivered for other projects.

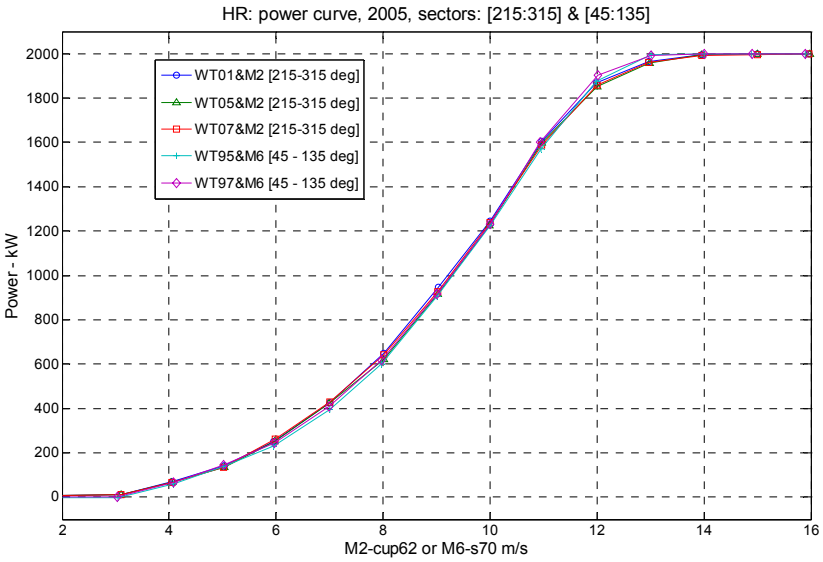

Figure 3: Power curves during unstable conditions.

Table 3: Reference power curve for V80 - located at Horns Rev, during unstable atmospheric conditions.

V_{hub} (m/s)	Power (kW)
5.5	184.8
6.5	324.8
7.5	511.7
8.5	751.0
9.5	1048.4
10.5	1409.5

2.3.3 Definition of reference wind direction

The wind direction is measured both at the three masts and as the nacelle position of each individual wind turbine. According to [1], it is rather difficult to use one of these values and based on this reference it was decided to use an upstream wind turbine as reference. The nacelle position of wt07 has been used as a reference with a mean offset correction of 21 degrees.

2.3.4 Methodology

The data query has been performed on the 10 minute mean electrical power values where:

- $5.5<V_{hub}\leq 6.5$ m/s equals $185<$El.Power≤ 325 kW for the upwind wind turbine
- $7.5<V_{hub}\leq 8.5$ m/s equals $510<$El.Power≤ 750 kW for the upwind wind turbine
- $9.5<V_{hub}\leq 10.5$ m/s equals $1050<$El.Power≤ 1410 kW for the upwind wind turbine

The resulting mean power output from both upwind and downwind turbines are transformed to wind speed by use of the reference power curve given in Table 3.

2.3.5 Conditions used for the data selection

A number of predefined conditions have been applied to the data search criteria for each of the three flow cases defined in section **Error! Reference source not found.**:

1. The power from the upwind column of wind turbines have been used to determine the wind speed level, while there is no free, undisturbed wind speed signals available nearby.
2. The atmospheric stability (z/L) is based on only an air/air temperature difference, measured at wake mast M7, due to lack of valid observations from other masts.
3. The directional bin size is 2 degrees, with reference to the nacelle direction wt07.
4. The number of required, online wind turbines in each row has been limited to 8 (e.g. wt0x, wt1x, wt2x, wt3x, wt4x, wt5x, wt6x & wt7x), where x is the row number.
5. The number of online wind turbines in each diagonal is 5 (e.g. wt07, wt16, wt25, wt34 & wt43).

2.3.6 Turbulence intensity

Unfortunately the turbulence intensity measured at hub height on a free, undistrubed mast (M2), was not available during the period. The mean turbulence intensity measured during 2 previous years has been extracted, corresponding to each flow case and wind speed bin, as shown on Figure 4, but the turbulence intensity is not sorted according to atmospheric stability.

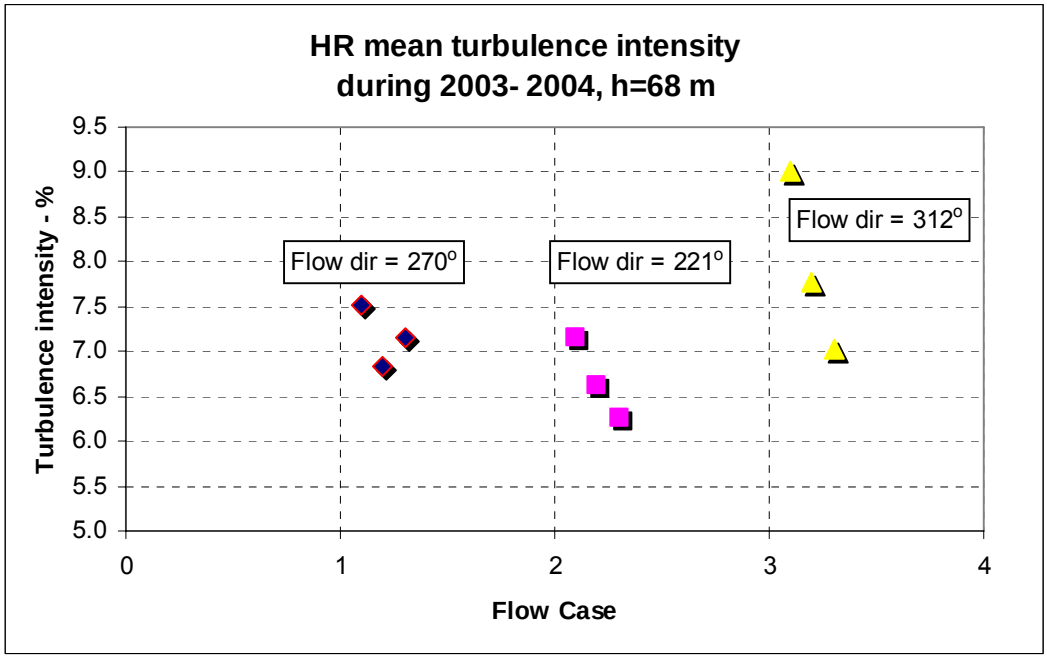

Figure 4: Turbulence intensity at Horns Rev as function of wind speed bin and wind direction recorded during 2003 - 2004.

2.4 Case 1: flow direction 270 degrees with a 7D spacing.

The flow direction 270 degrees is along rows of 10 wind turbines with 7D spacing, but only 8 upwind turbines in each row have been included in the wake deficit determination.

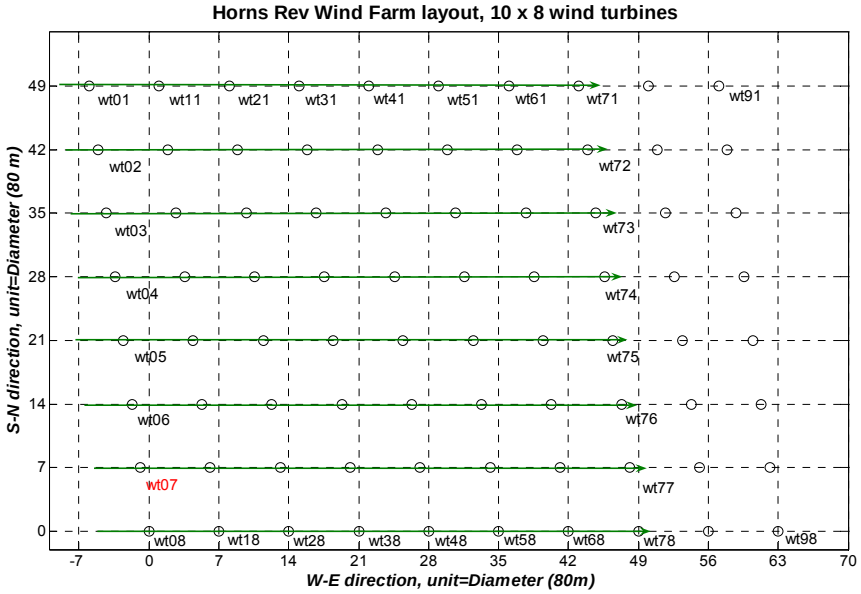

Figure 5: Flow direction in case 1; 8x8 rows of online turbines are used in this flow case, with reference to turbine wt07.

Table 4: Definition of Case 1.

Case	Speed	Direction	Stratification	Valid periods
1.6.1	6 ±0.5 m/s	270°±1	-12<z/L≤-2	8/row
1.6.2	6 ±0.5 m/s	270°±5	z/L≤-12	8/row
1.6.3	6 ±0.5 m/s	270°±5	-12<z/L≤-2	45/row
1.6.4	6 ±0.5 m/s	270°±5	-2<z/L≤+2	15/row
1.6.5	6 ±0.5 m/s	270°±5	2<z/L	6/row
1.6.6	6 ±0.5 m/s	270°±10	-12<z/L≤-2	64/row
1.6.7	6 ±0.5 m/s	270°±15	-12<z/L≤-2	120/row
1.8.1	8 ±0.5 m/s	270°±1	-12<z/L≤-2	8.6/row
1.8.2	8 ±0.5 m/s	270°±5	-12<z/L≤-2	54/row
1.8.3	8 ±0.5 m/s	270°±10	-12<z/L≤-2	113/row
1.8.4	8 ±0.5 m/s	270°±15	-12<z/L≤-2	156/row
1.10.1	10 ±0.5 m/s	270°±1	-12<z/L≤-2	3.5/row
1.10.2	10 ±0.5 m/s	270°±5	-12<z/L≤-2	16/row
1.10.3	10 ±0.5 m/s	270°±10	-12<z/L≤-2	25/row
1.10.4	10 ±0.5 m/s	270°±15	-12<z/L≤-2	36/row

Comments: Only a limited number of available observations have been identified for each wind speed bin and stability class. Unstable and neutral stratification is dominating, as indicated on

Figure 2, se Case 1.6.3 and 1.6.4. Table 4 includes 2, 10, 20 & 30 degree sector results suitable for WAsP flow modeling. The flow deficit is presented both as a power deficit ratio and as a derived speed deficit with reference to the upwind turbine. The deficits are listed in Appendix C.

2.4.1 Flow profiles for case 1

Case 1.6; wind speed bin at 6 m/s results in 15 x 8 periods = 120 periods distributed on 8 rows, which corresponds to approximately 2 hour of valid measurements along each row for a 2 degree sector. The mean wind speed deficit along a row is presented as function of the distance between upwind and downwind wind turbine for each case. The error bars represents the standard deviation of the mean row deficits (8 rows).
Case 1.6.1, 1.6.3, 1.6.6 and 1.6.7 are plotted together for comparison and the deficits are listed in Appendix C.

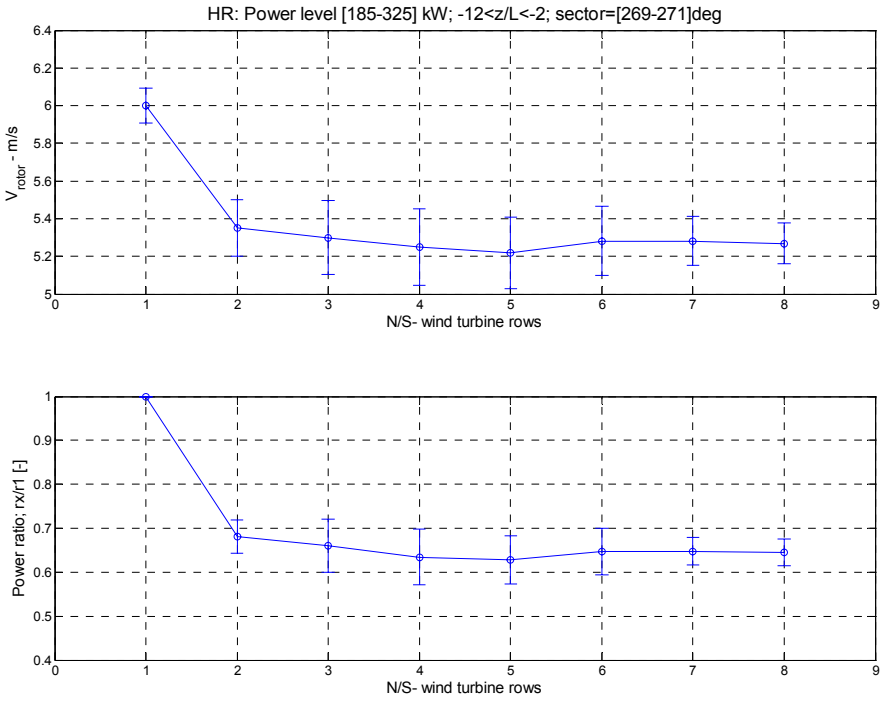

Figure 6: Case 1.6.1; Speed and power deficit at 6 m/s during unstable conditions, sector=2 deg.

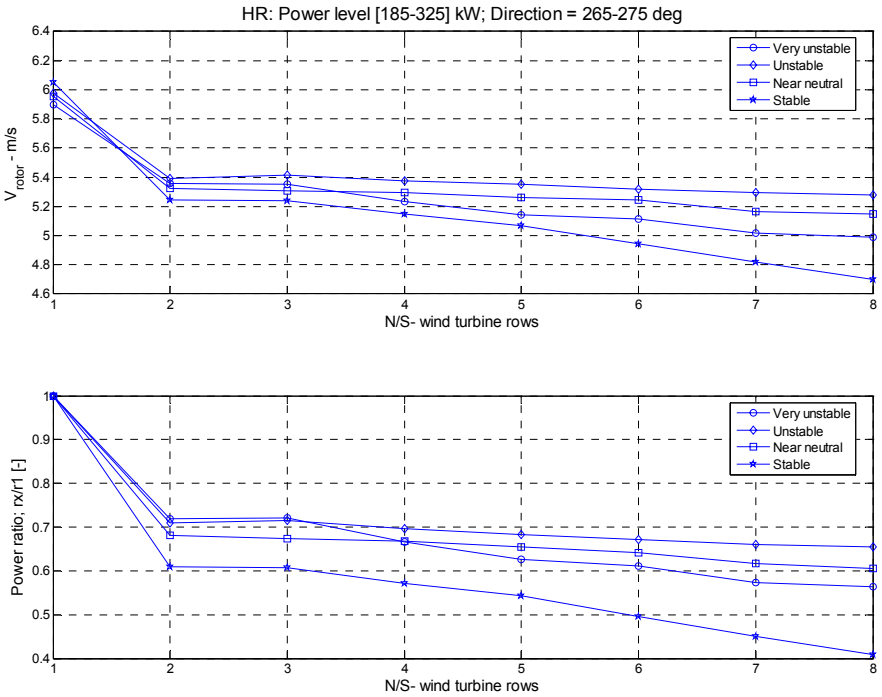

Figure 7: Speed and power deficit at 6 m/s during very unstable, unstable, neutral and stable conditions, sector=10 deg.

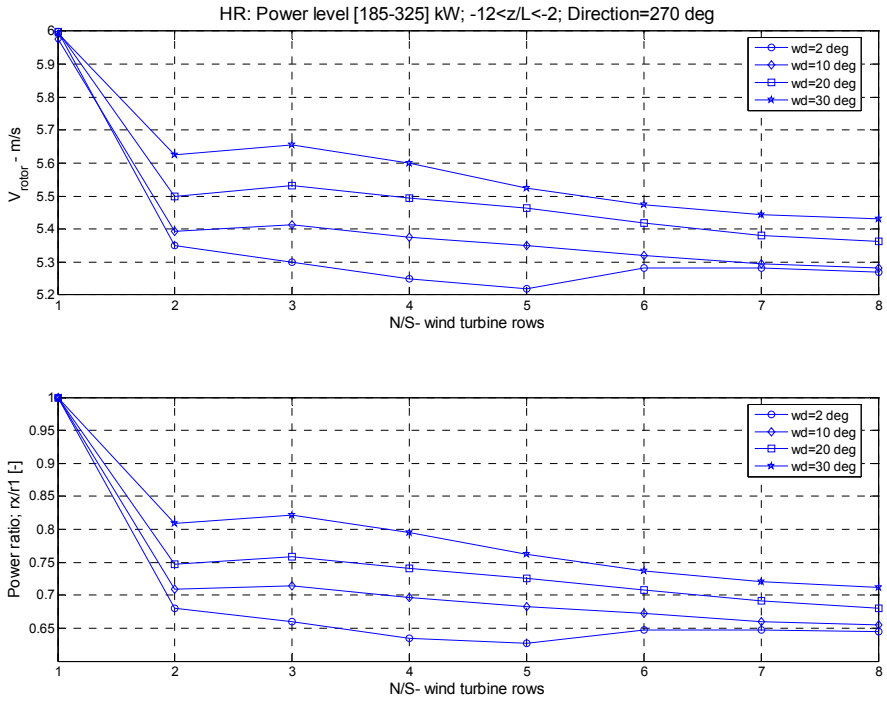

Figure 8: Speed and power deficit at 6 m/s during unstable conditions, for sectors = 2, 10, 20 & 30 deg.

Case 1.8; wind speed bin at 8 m/s results in 20 x 8 periods = 160 periods distributed on 8 rows, which corresponds to approximately 3 hour of valid measurements along each row for a 2 degree sector. The mean wind speed deficit along a row is presented as function of the distance between upwind and downwind wind turbine for each case.

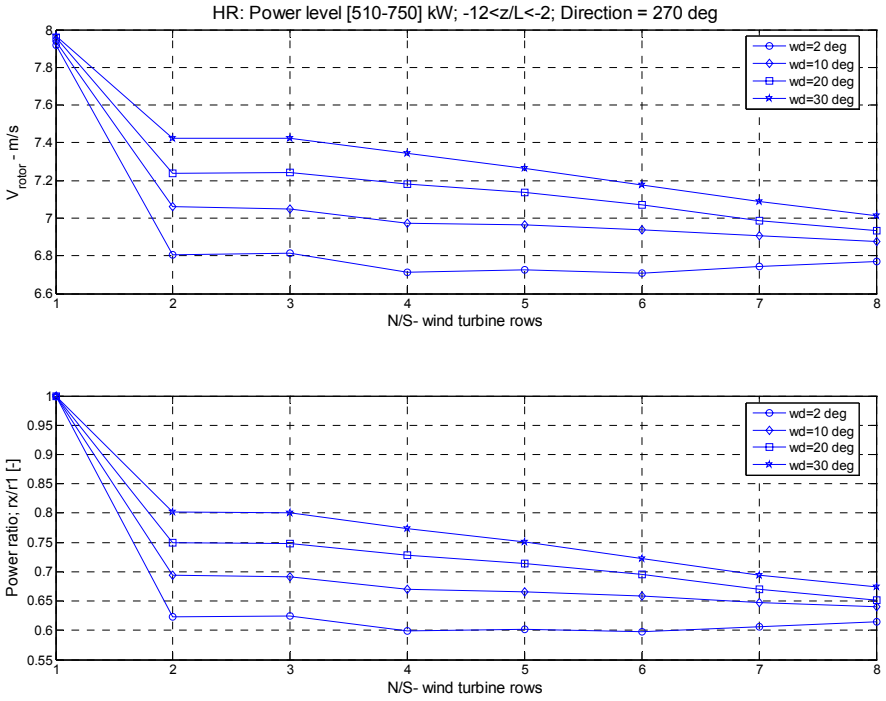

Figure 9: Speed and power deficit at 8 m/s during unstable conditions, sectors = 2, 10, 20 & 30 deg.

A detailed directional sensitivity analysis has been performed for 2 degree sector observations covering both unstable and near neutral conditions. The figure, which is shown in Appendix B, demonstrates how sensitive the speed deficit is to the “pure” wake situation (sector = 169-271 deg.).

Case 1.10; wind speed bin at 10 m/s results in 16.5 x 8 periods = 138 periods distributed on 8 rows, which corresponds to approximately 3 hours of valid measurements along each row for a 2 degree sector. The mean wind speed deficit along a row is presented as function of the distance between upwind and downwind wind turbine for each case.

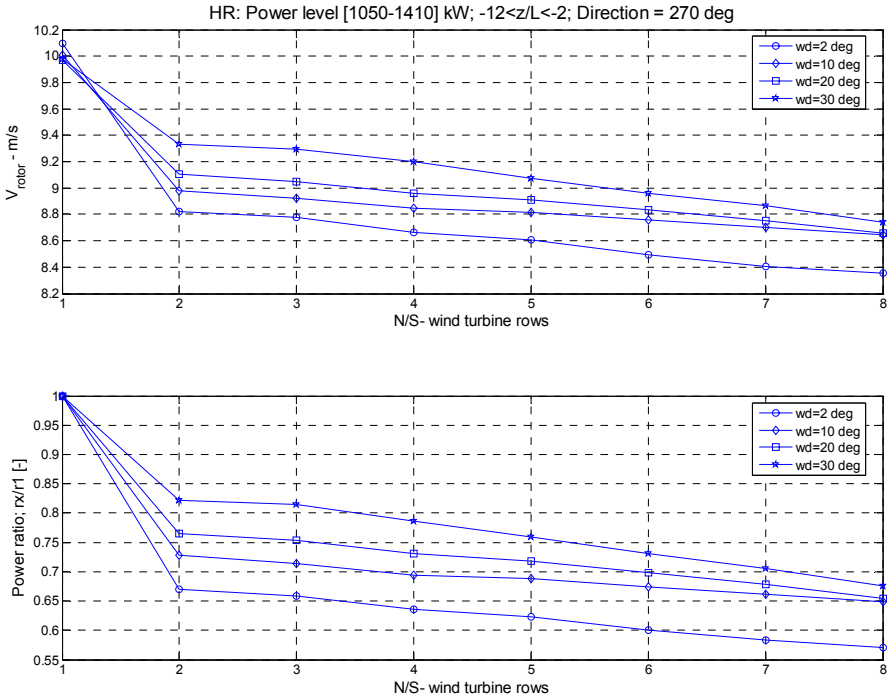

Figure 10: Speed and power deficit at 10 m/s during unstable conditions, sectors = 2, 10, 20 and 30 deg.

2.5 Case 2: flow direction 221 degrees diagonal through the wind farm with 9.4D spacing.

The flow direction 221 degrees is along rows of 5-10 wind turbines with 9.4D spacing, where 5 turbines in each row are included in the wake deficit determination.

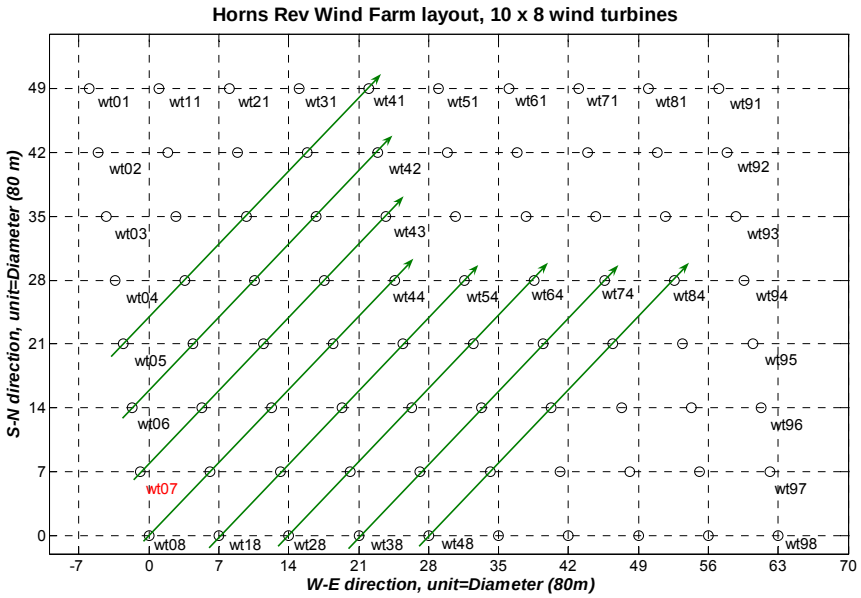

Figure 11: Flow direction in Case 2, 8x 5 rows of online turbines are used in this case, with reference to wt07.

The wake deficits determined in Case 2 is based on measurements from 8 diagonal rows each consisting of 5 wind turbines, as indicated on Figure 11.

Table 5: Definition of Case 2.

Case	Speed	Direction	Stratification	Valid periods
2.6.1	6 ±0.5 m/s	221°±1	z/L≤-12	0.6/row
2.6.2	6 ±0.5 m/s	221°±1	-12<z/L≤-2	3/row
2.6.3	6 ±0.5 m/s	221°±1	-2<z/L≤+2	5/row
2.6.4	6 ±0.5 m/s	221°±1	+2<z/L	6/row
2.6.5	6 ±0.5 m/s	221°±5	-12<z/L≤-2	18/row
2.6.6	6 ±0.5 m/s	221°±10	-12<z/L≤-2	32/row
2.6.7	6 ±0.5 m/s	221°±15	-12<z/L≤-2	49/row
2.8.1	8 ±0.5 m/s	221°±1	-12<z/L≤-2	12/row
2.8.2	8 ±0.5 m/s	221°±5	-12<z/L≤-2	48/row
2.8.3	8 ±0.5 m/s	221°±10	-12<z/L≤-2	84/row
2.8.4	8 ±0.5 m/s	221°±15	-12<z/L≤-2	106/row
2.10.1	10 ±0.5 m/s	221°±1	-12<z/L≤-2	1/row
2.10.2	10 ±0.5 m/s	221°±5	-12<z/L≤-2	4.6/row
2.10.3	10 ±0.5 m/s	221°±10	-12<z/L≤-2	8.6/row
2.10.4	10 ±0.5	221°±15	-12<z/L≤-2	16/row

m/s

Table 5 defines 2, 10, 20 and 30 degree flow sectors suitable for WAsP flow modeling and the deficits are listed in Appendix C.

2.5.1 Flow profiles for case 2

Case 2.6; wind speed bin at 6 m/s results in 13 x 8 periods =104 periods distributed on 8 rows, which corresponds to approximately 2 hours of valid measurements along each row for a 2 degree sector. The mean wind speed deficit along a row is presented as function of the distance between upwind and downwind wind turbine for each case.

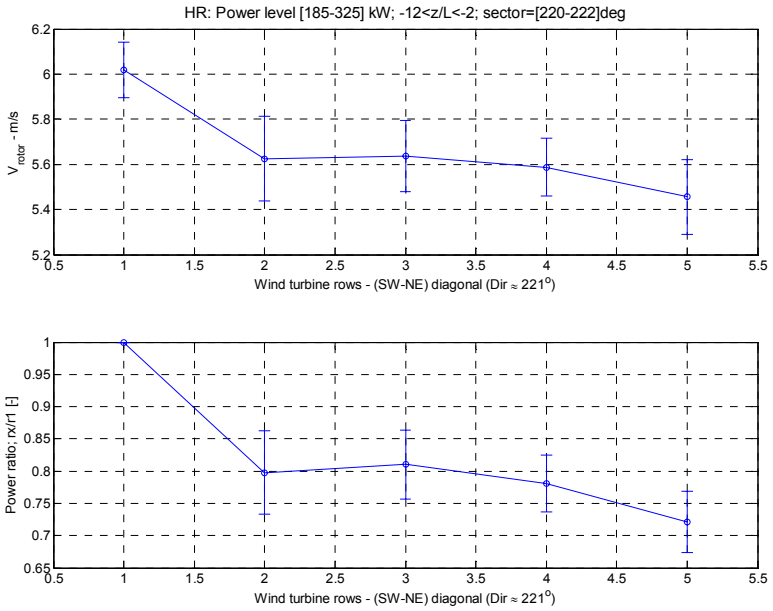

Figure 12: Case 2.6.2; Speed and power deficit at 6 m/s during unstable conditions, sector=2 deg.

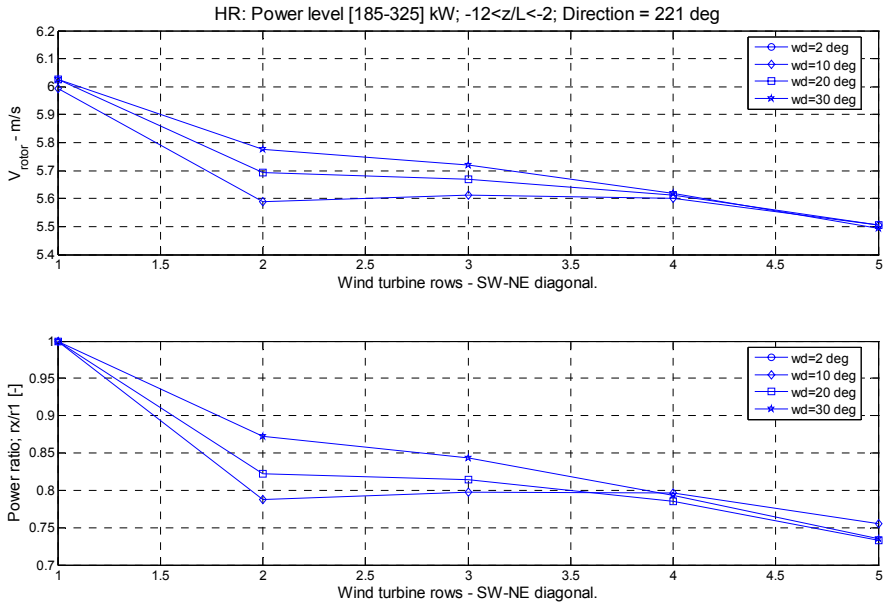

Figure 13: Speed and power deficit at 6 m/s during unstable conditions, sector=10, 20 & 30 deg.

Case 2.8; wind speed bin at 8 m/s results in 22 x 8 periods =176 periods distributed on 8 rows, which corresponds to approximately 3½ hours of valid measurements along each row for a 2 degree sector. The mean wind speed deficit along a row is presented as function of the distance between upwind and downwind wind turbine for each case.

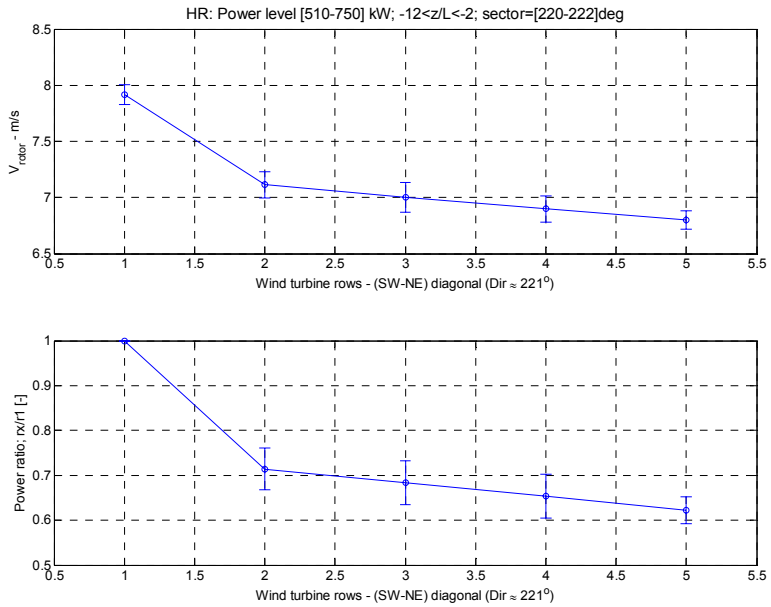

Figure 14: Case 2.8.1; Speed and power deficit at 8 m/s during unstable conditions, sector=2 deg, based on 12 periods.

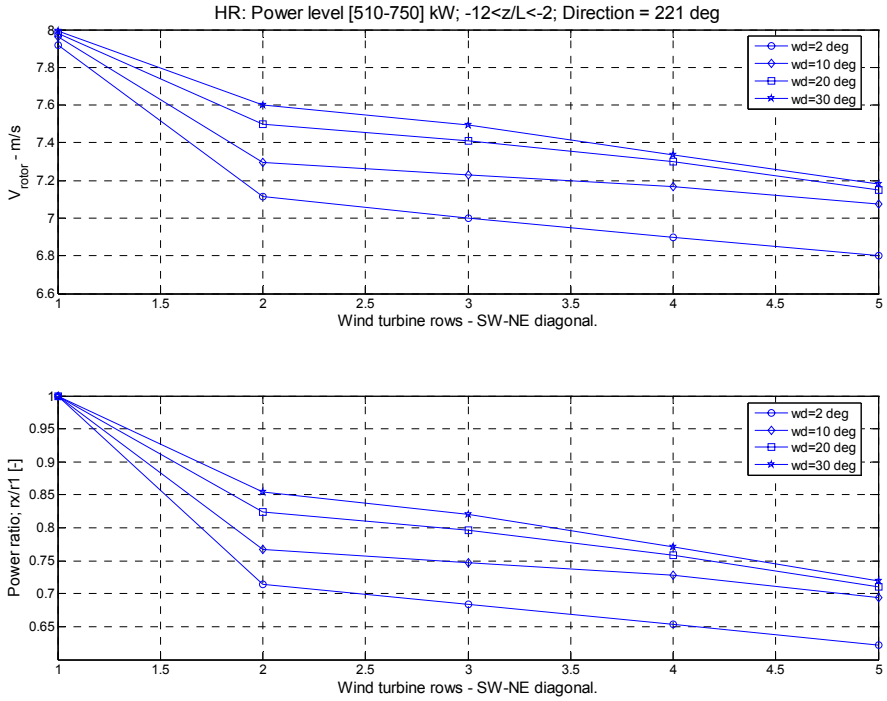

Figure 15: Speed and power deficit at 8 m/s during unstable conditions, sector= 2, 10, 20 & 30 deg.

Case 2.10; wind speed bin at 10 m/s results in 23 x 8 periods =184 periods distributed on 8 rows, which corresponds to 4 hours of valid measurements along each row for a 2 degree sector. The mean wind speed deficit along a row is presented as function of the distance between upwind and downwind wind turbine for each case.

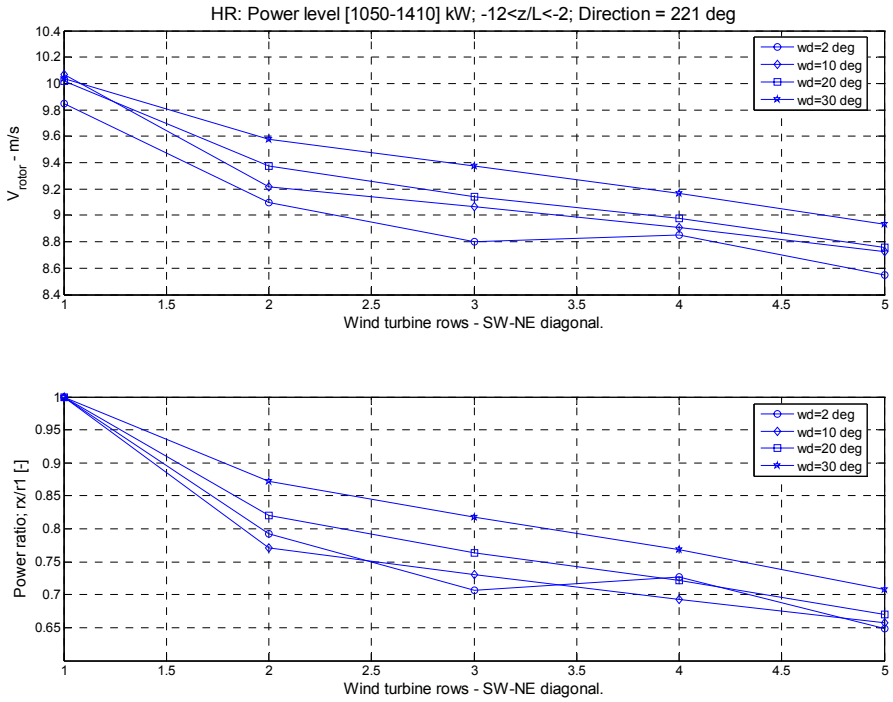

Figure 16: Speed and power deficit at 10 m/s during unstable conditions, sector=2, 10, 20 & 30 deg.

2.6 Case 3: flow direction 312 degrees with 10.4D spacing.

The flow direction 312 degrees is along a row of 5-10 wind turbines with a 10.4D spacing, where 5 turbines in each row are included in the wake deficit determination.

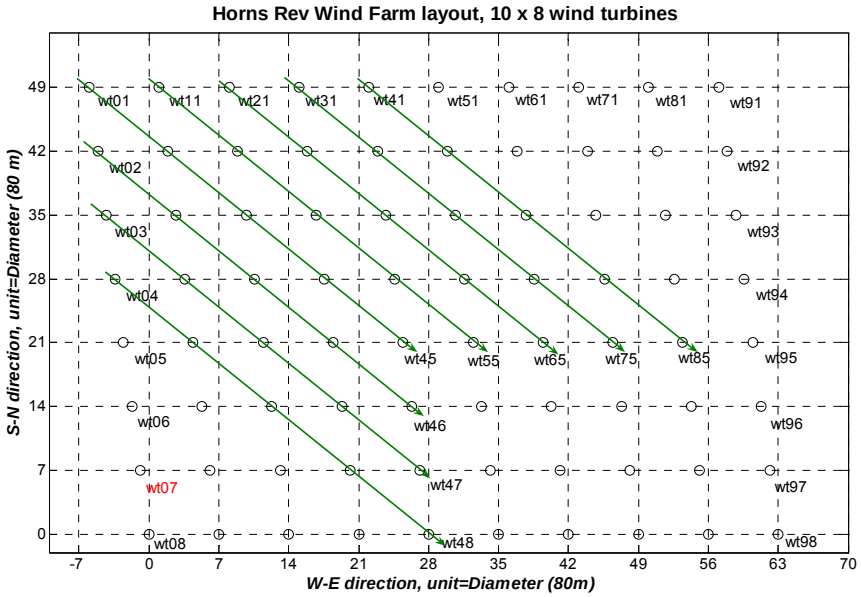

Figure 17: Flow directions used in case 2, 7x 5 online turbines are used with reference to wt07.

The wake deficits determined in Case 3 is based on measurements from 8 diagonal rows each consisting of 5 wind turbines, as indicated on Figure 17.

Table 6: Definition of Case 3.

Case	Speed	Direction	Stratification	Valid periods
3.6.1	6 ±0.5 m/s	312°±1	z/L≤-12	0/row
3.6.2	6 ±0.5 m/s	312°±1	-12<z/L≤-2	16/row
3.6.3	6 ±0.5 m/s	312°±1	-2<z/L≤2	1/row
3.6.4	6 ±0.5 m/s	312°±1	z/L>2	2/row
3.6.5	6 ±0.5 m/s	312°±5	-12<z/L≤-2	70/row
3.6.6	6 ±0.5 m/s	312°±10	-12<z/L≤-2	120/row
3.6.7	6 ±0.5 m/s	312°±15	-12<z/L≤-2	171/row
3.8.1	8 ±0.5 m/s	312°±1	-12<z/L≤-2	5/row
3.8.2	8 ±0.5 m/s	312°±5	-12<z/L≤-2	26/row
3.8.3	8 ±0.5 m/s	312°±10	-12<z/L≤-2	54/row
3.8.4	8 ±0.5 m/s	312°±15	-12<z/L≤-2	94/row
3.10.1	10 ±0.5 m/s	312°±1	-12<z/L≤-2	2/row
3.10.2	10 ±0.5 m/s	312°±5	-12<z/L≤-2	9/row
3.10.3	10 ±0.5 m/s	312°±10	-12<z/L≤-2	22/row
3.10.4	10 ±0.5 m/s	312°±15	-12<z/L≤-2	28/row

Table 6 includes 2, 10, 20 and 30 degree sector results, suitable for WAsP flow modeling and the deficits are listed in Appendix C.

2.6.1 Flow profiles for case 3

Case 3.6; wind speed bin at 6 m/s results in 20 x 8 periods =160 periods distributed on 8 rows, which corresponds to approximately 3 hours of valid measurements along each row for a 2 degree sector. The mean wind speed deficit along a row is presented as function of the distance between upwind and downwind wind turbine for each case.

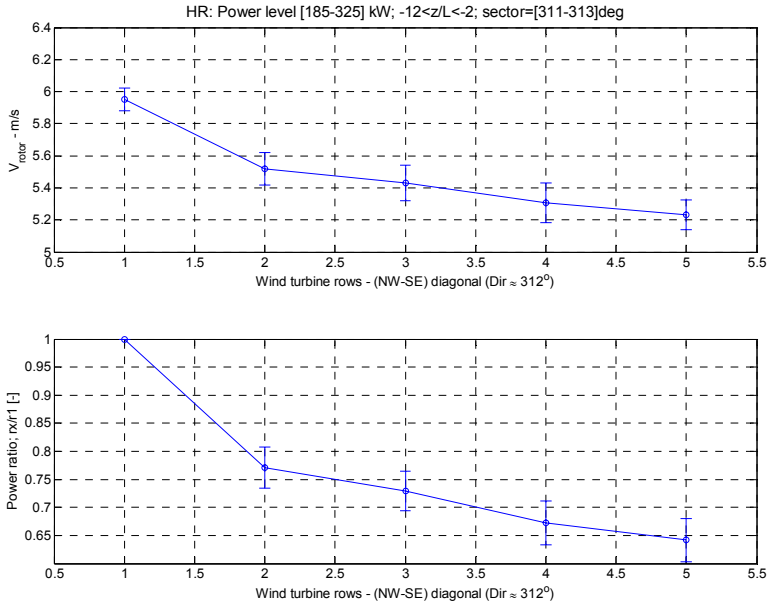

Figure 18: Case 3.6.2, Speed and power deficit at 6 m/s during unstable conditions, sector=2 deg.

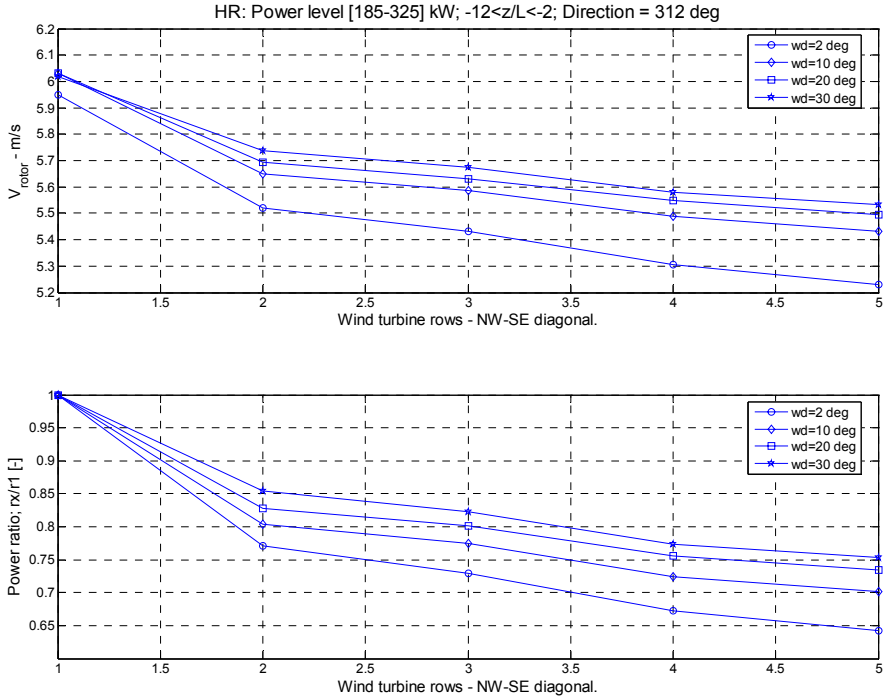

Figure 19: Speed and power deficit at 6 m/s during unstable conditions, sector = 2, 10, 20 and 30 deg.

Case 3.8; wind speed bin at 8 m/s results in 13 x 8 periods =104 periods distributed on 8 rows, which corresponds to 2 hours of valid measurements along each row for a 2 degree sector. The mean wind speed deficit along a row is presented as function of the distance between upwind and downwind wind turbine for each case.

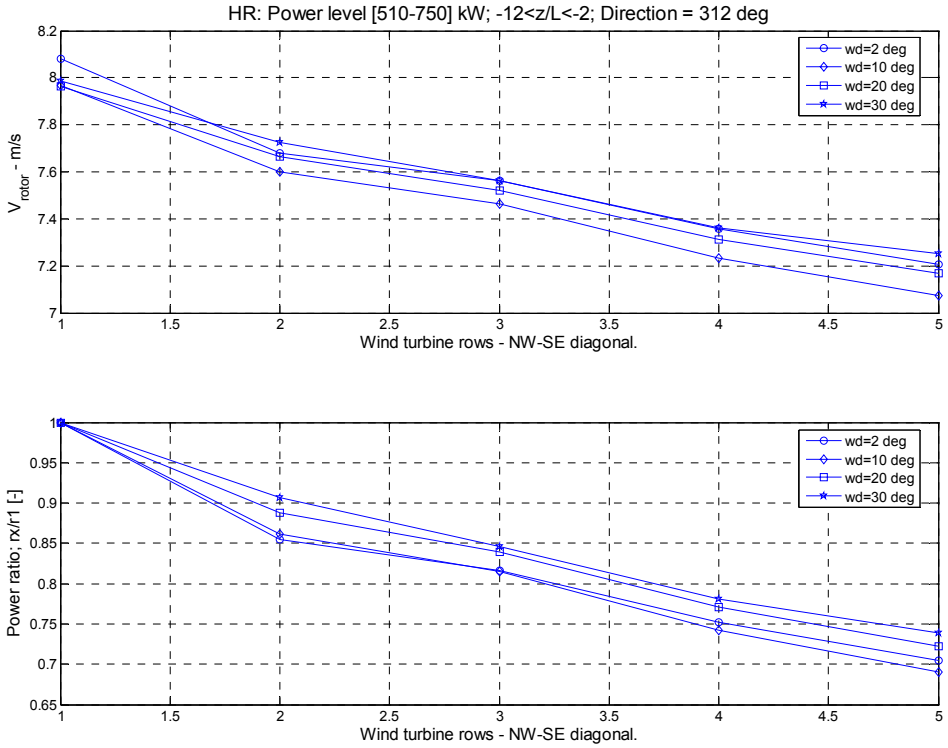

Figure 20: Speed and power deficit at 8 m/s during unstable conditions, sector = 2, 10, 20 & 30 deg.

Case 3.10; wind speed bin at 10 m/s results in 26.6 x 8 periods =213 periods distributed on 8 rows, which corresponds to approximately 5 hours of valid measurements along each row for a 2 degree sector. The mean wind speed deficit along a row is presented as function of the distance between upwind and downwind wind turbine for each case.

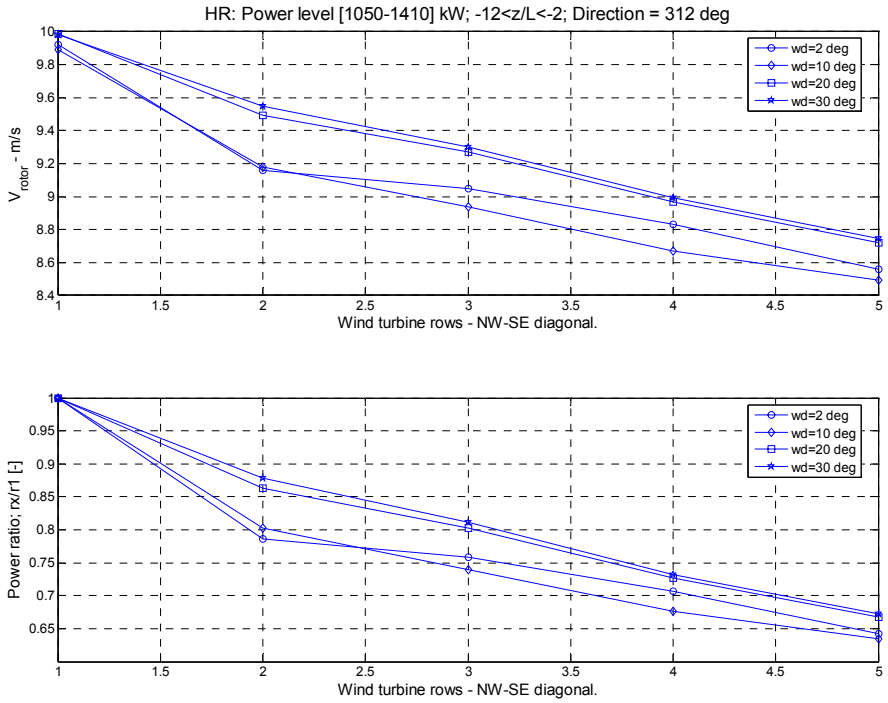

Figure 21: Speed and power deficit at 10 m/s during unstable conditions, sector = 2, 10, 20 & 30 deg.

2.7 Discussion

The finding from basic flow cases have been presented above both as power deficit ratios and as derived wind speed deficits. The major findings are:

- The smallest sector size of 2° represents an almost “pure” wake situation where all downwind turbines are covered by the wake, which is demonstration by a very low (<0.5°) mean yaw misalignment of the down wind turbines.
- The uncertainty of the nacelle position value is rather low, which influences the quality resulting mean deficit. Furthermore all nacelle position registrations are uncorrected due to an individual varying offset.
- Increased sector size of 10, 20 and 30 degrees decreases the deficit due to increased mixing and meandering wakes.
- The uncertainty of the power measurements is unknown, while there is now available documentation on sensor calibration, measurement chain setup,...
- Due to high uncertainty both on the temperature difference recordings and wind speed differences inside the wind farm wake, the derived stability measure is rather uncertain, which influences the deficit determination as function of stability.

- Several sub-cases contain only a limited number of valid observations, which influences the contents of the final flow cases matrix.

3. Complex terrain

3.1 Overview

Models of the engineering type have been developed and calibrated for flat terrain applications. However, in complex terrain applications, the assumptions made in those models are no longer valid. More advanced methods should be applied taking into account the effect of the atmospheric boundary layer including flow separation and streamlining. In this respect the adoption of Navier-Stokes solvers seems to be the most accurate approach and the only one capable of simulating the interaction of wind turbine wake with the wind velocity shear and the shape of the complex terrain.

There are several issues, which need to be investigated regarding wake modelling in complex terrain:

- Complex topography results in the narrowing of the wind rose and the decrease the Weibull-k values. How does the narrowing behave with the increase in the hub height? The effect on the power curve should be quantified.
- The effect of topography on the wake geometry has to be investigated. Does the wake follow the streamlines? How does the terrain affect the wake opening?
- The reference wind velocity should be correctly assigned for modelling purposes. This is not obvious for steep slopes and wind parks with machine-wake interaction. In the context of an actuator disk modelling of the wind turbines, the combination of a BEM method with a Navier-Stokes solver could overcome the issue of the reference velocity definition by directly calculating the blade forces.

By answering these issues, it is expected to develop relationships for the maximum wind velocity deficit, the turbulence intensity and the wake geometry, which would complete the wake modelling along with those existing in flat terrain.

3.2 Complex terrain cases: Gaussian Hill

The idealized simulation of a single wake in the case of a Gaussian hill will constitute the basis for the comparison of the wake characteristics between flat and complex terrain. The conclusions deduced from the analysis of the 3D and 2D Gaussian hill can be extended to more complex terrain where the irregularities of the topography are seen as separate hills.

The Gaussian 2D hill geometry is defined by the relationship

$$z = h\, e^{\left[-0.5\left(\frac{x}{\sigma}\right)^2\right]},\ \sigma = L/1.1774, \qquad (1)$$

here x, z are the horizontal and vertical coordinates, h is the height of the hill and L is defined as $x(z = h/2)$. In the 3D hill, $\sqrt{x^2 + y^2}$ replaces x in Eq.(1). The 3D and 2D hill terrain derived from Eq.(1) for $L = 1750$ are shown in Fig.1. Two configurations corresponding to different hill slopes will be examined: $h = 700m$, $L = 1750m$ (steep slope) and $h = 700m$, $L = 3000m$ (gentle slope).

The different configurations will be simulated with one wind turbine at hilltop and without the wind turbine. The simulations without the wind turbine are needed to provide the value of wind speed at the wind turbine position for the calculation of the actuator disk force as well as the reference velocity field for the evaluation of the wind speed deficit. The machine is the 5 MW reference turbine used in Upwind WP2 with 126 m diameter (D=126 m) and 90 m hub height. Note, that the lengths in Figure 22 have been dimensionalized with the wind turbine diameter. The input wind velocity profile is assumed logarithmic with 500 m boundary layer height and

10m/s velocity at hub height. Three different levels of turbulence intensity (5%, 13% and 15%) and six different wind directions (0, ±15°, ±30°) will be examined.

The variations of wind speed deficit and turbulence intensity at hub height above ground level and the vertical profiles behind the wind turbine must be estimated and compared to the respective ones in flat terrain, so that basic guidelines are derived for the effect of the hill on the wake characteristics.

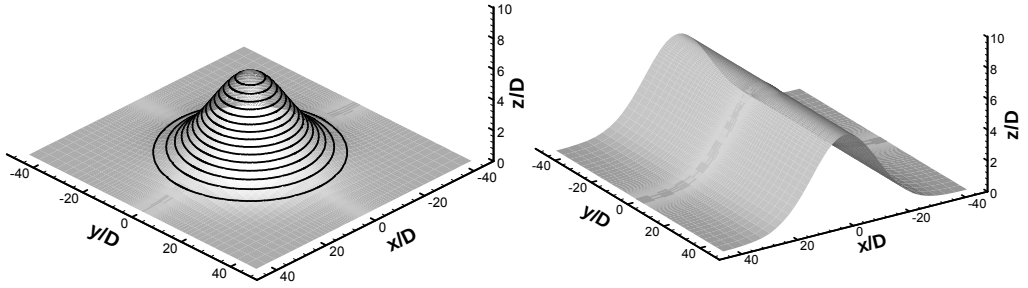

Figure 1: Terrain of the 3D and 2D Gaussian hill ($L = 1750$).

3.3 Complex terrain cases: five turbines in flat terrain

In flat terrain wind parks, wind turbines are often aligned in parallel rows, which means that one machine can be partially or completely situated in the wake of a neighbouring wind turbine. In order to estimate the effect of a neighbouring wake on the wind turbine efficiency, multi-wake simulations for the worst (in terms of efficiency) case will be examined.

The simulation of five subsequent wind turbines in flat terrain is considered to well cover this case. A parametric analysis will be done for different values of the distance between the wind turbines (3, 5 and 7D) and different values of Ct (0.3, 0.5 and 0.7). The level of turbulence intensity will be set equal to 13%.

The wind speed deficit and wake radius variations at hub height will indicate the significance of the wake effect of the previous wind turbines and how this effect decays as the distance from the first machine increases. The vertical and lateral profiles of the wind deficit along with the xz and yz contour plots can represent the evolution of the wake geometry.

3.4 Complex terrain cases: the complex terrain wind farm

A real wind farm located in a moderately complex terrain is proposed for the comparison and validation of wake models. The wind farm, installed in 2001, is constituted by 43 wind turbines separated 1.5 diameters in the adjacent direction and approximately 11 diameters between rows. The layout is formed by 5 alignments oriented towards the prevailing wind directions (NW-SE).

Two meteorological masts are located upstream of the wind farm on the wind directions mentioned above. The masts registered 10 minutes averages of wind speed, wind direction and standard deviation of wind speed at 20 m and 40 m high. In addition, the air temperature is measured at 10 m height. Regarding power data, the output energy as well as the nacelle wind speed for every wind turbine is recorded on an hourly basis. Furthermore, a specific status signal is also registered in order to filter the unavailability of the wind turbines. Overall, a 2 year period of simultaneous data (meteorological and wind farm) is available.

The location of the meteorological masts allows the upstream flow in the prevailing wind direction to be characterised in order to analyse situations of far wake. Other non-prevailing

sectors (W-WSW) corresponding to near wake scenarios are known to contain enough frequency of data and some information could also be extracted. Yaw angle at the wind turbines was not registered so that only wind direction at the meteorological masts could be used at the filtering process.

The study represents a first attempt of comparing and validating the existing wake models on a real moderately complex site and according to real field data.

4. Acknowledgement

We would like to acknowledge DONG Energy A/S (formerly ELSAM Engineering A/S) and Vattenfall AB, owners of the Horns Rev wind, the owners of the wind farm in complex terrain and the five turbines in flat terrain for allowing use of their data.

5. References.

[1] "Investigation of Observed and Modeled Wake Effect on Horns Rev", using WindPro; Master thesis made by David Ryan Van Luvanee; MEK, DTU 2006,
[2] Upwind WP8 kick-off meeting 17.10.2006, Aristo, Amsterdam
[3] Leo E. Jensen et.al.”Wake measurements from the Horns Rev Wind farm”, presented at EWEC 2004, London, November 2004

Appendix A: Location of meteorological mast at the Horns Rev wind farm.

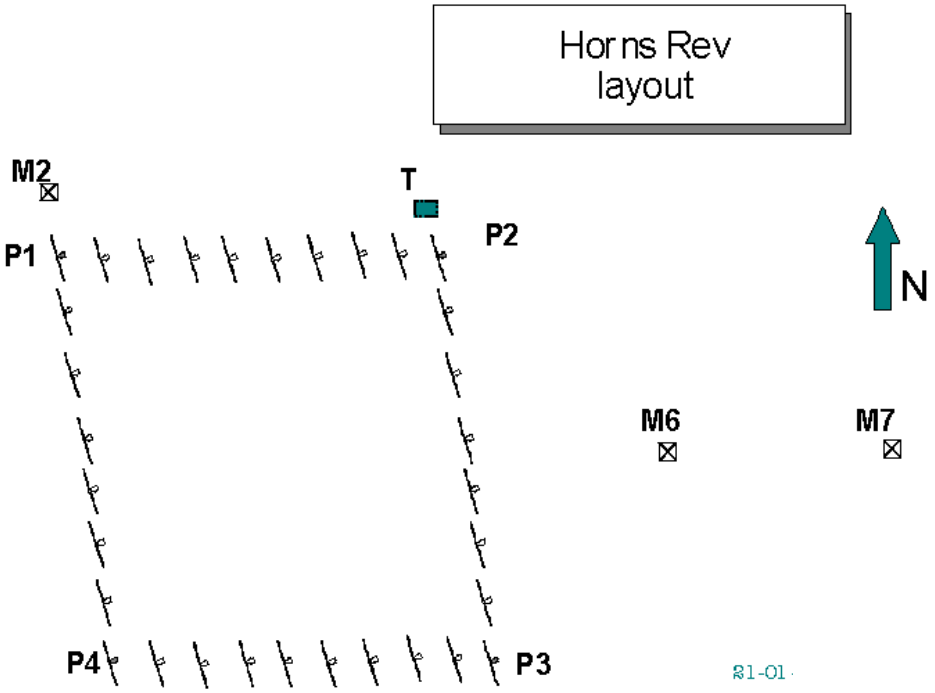

Position of main objects:

- The park corners turbines are P1 (=wt01), P2 (=wt91), P3 (=wt98) and P4 (=wt08)
- Transformer stations T, is located NW of P2
- Mast M2 is located NW of the P1,
- Mast M6 is located 2 km east of the park
- Mast M7 is located 6 km east of the park

	Coordinates	
M2	423.41	6153.3
P1	423.97	6151.4
P2	429.01	6151.4
P3	429.45	6147.6
P4	424.45	6147.6
T	428.95	6152.0
M6	431.25	6149.5
M7	435.25	6149.5

Direction between main objects

directions, deg	M2	M6	M7
P1	163	285	280
P2	109	311	287
P3	134	227	251
T	104	317	292
M6	116	0	270
M7	108	90	0
M2	0	296	288

Free inflow sectors to masts

	Mast	
M2	0°	90°
M2	180°	360°
M6	-20°	200°
M7	-40°	220°

Appendix B: Directional sensitivity analysis for Case 1.8.2

The wake deficit as function of wind direction for a number of 2 degrees sectors has been determined for the 7D flow case, where each curve represents approximately 3 hours of measurements.

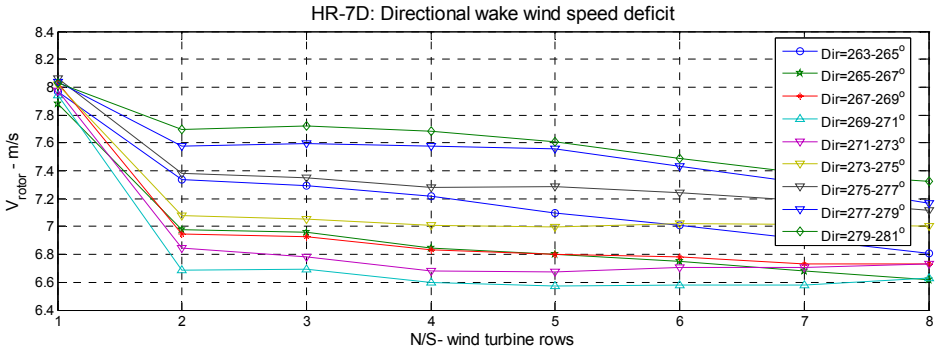

Figure 22: Directional wake deficits during unstable and near neutral conditions, V_{hub}=8 ±0.5 m/s.

Appendix C: Calculated speed and power deficit values

	CASE:1.6 - Figure 8							
	speed deficit				**power deficit ratio**			
row	*dw=2o*	*dw=10o*	*dw=20o*	*dw=30o*	*dw=2o*	*dw=10o*	*dw=20o*	*dw=30o*
1	6.00	5.97	6.00	5.99	1.000	1.000	1.000	1.000
2	5.35	5.39	5.50	5.62	0.681	0.709	0.747	0.808
3	5.30	5.41	5.53	5.66	0.660	0.715	0.759	0.822
4	5.25	5.37	5.49	5.60	0.634	0.696	0.741	0.795
5	5.22	5.35	5.46	5.52	0.627	0.682	0.725	0.762
6	5.28	5.32	5.42	5.47	0.648	0.672	0.708	0.737
7	5.28	5.29	5.38	5.44	0.648	0.659	0.691	0.720
8	5.27	5.28	5.36	5.43	0.645	0.654	0.680	0.712

	CASE:1.8 - Figure 9							
	speed deficit				**power deficit ratio**			
row	*dw=2o*	*dw=10o*	*dw=20o*	*dw=30o*	*dw=2o*	*dw=10o*	*dw=20o*	*dw=30o*
1	7.92	7.94	7.96	7.97	1.000	1.000	1.000	1.000
2	6.81	7.06	7.24	7.42	0.623	0.694	0.750	0.802
3	6.81	7.05	7.24	7.42	0.625	0.691	0.749	0.801
4	6.71	6.97	7.18	7.34	0.599	0.671	0.728	0.774
5	6.72	6.96	7.14	7.26	0.601	0.665	0.714	0.750
6	6.71	6.94	7.07	7.17	0.598	0.659	0.695	0.723
7	6.74	6.91	6.99	7.09	0.607	0.647	0.670	0.694
8	6.77	6.87	6.93	7.01	0.615	0.640	0.652	0.675

	CASE:1.10 - Figure 10							
	speed deficit				**power deficit ratio**			
row	*dw=2o*	*dw=10o*	*dw=20o*	*dw=30o*	*dw=2o*	*dw=10o*	*dw=20o*	*dw=30o*
1	10.09	10.01	9.97	9.98	1.000	1.000	1.000	1.000
2	8.82	8.98	9.11	9.33	0.669	0.728	0.765	0.822
3	8.77	8.92	9.05	9.29	0.659	0.714	0.754	0.814
4	8.66	8.84	8.96	9.20	0.636	0.694	0.731	0.787
5	8.61	8.81	8.91	9.07	0.623	0.688	0.719	0.759
6	8.49	8.76	8.83	8.96	0.600	0.674	0.698	0.731
7	8.41	8.70	8.75	8.86	0.584	0.662	0.678	0.706
8	8.36	8.64	8.66	8.74	0.571	0.649	0.654	0.676

	CASE 2.6 - Figure 13							
	speed deficit				**power deficit ratio**			
row	*dw=2o*	*dw=10o*	*dw=20o*	*dw=30o*	*dw=2o*	*dw=10o*	*dw=20o*	*dw=30o*
1		5.99	6.02	6.02		1.000	1.000	1.000
2		5.59	5.69	5.77		0.788	0.822	0.873
3		5.61	5.67	5.72		0.797	0.814	0.844

4		5.60	5.61	5.62		0.797	0.785	0.793
5		5.51	5.51	5.49		0.756	0.732	0.735

	CASE 2.8 - Figure 15							
	speed deficit				**power deficit ratio**			
row	*dw=2o*	*dw=10o*	*dw=20o*	*dw=30o*	*dw=2o*	*dw=10o*	*dw=20o*	*dw=30o*
1	7.92	7.96	7.98	7.99	1.000	1.000	1.000	1.000
2	7.11	7.29	7.50	7.60	0.715	0.768	0.824	0.854
3	7.00	7.23	7.41	7.49	0.683	0.747	0.797	0.820
4	6.90	7.17	7.30	7.34	0.654	0.728	0.759	0.771
5	6.80	7.07	7.15	7.18	0.622	0.694	0.711	0.719

	CASE 2.10 - Figure 16							
	speed deficit				**power deficit ratio**			
row	*dw=2o*	*dw=10o*	*dw=20o*	*dw=30o*	*dw=2o*	*dw=10o*	*dw=20o*	*dw=30o*
1	9.85	10.07	10.02	10.04	1.000	1.000	1.000	1.000
2	9.10	9.22	9.38	9.58	0.792	0.771	0.820	0.872
3	8.80	9.06	9.14	9.38	0.706	0.730	0.763	0.817
4	8.85	8.91	8.97	9.17	0.726	0.693	0.721	0.768
5	8.55	8.72	8.76	8.93	0.648	0.658	0.670	0.708

	CASE 3.6 - Figure 19							
	speed deficit				**power deficit ratio**			
row	*dw=2o*	*dw=10o*	*dw=20o*	*dw=30o*	*dw=2o*	*dw=10o*	*dw=20o*	*dw=30o*
1	5.95	6.03	6.03	6.02	1.000	1.000	1.000	1.000
2	5.52	5.65	5.69	5.74	0.771	0.804	0.827	0.855
3	5.43	5.59	5.63	5.67	0.729	0.774	0.802	0.822
4	5.31	5.49	5.55	5.58	0.673	0.724	0.755	0.774
5	5.23	5.43	5.49	5.53	0.642	0.701	0.734	0.753

	CASE 3.8 - Figure 20							
	speed deficit				**power deficit ratio**			
row	*dw=2o*	*dw=10o*	*dw=20o*	*dw=30o*	*dw=2o*	*dw=10o*	*dw=20o*	*dw=30o*
1	8.08	7.97	7.96	7.99	1.000	1.000	1.000	1.000
2	7.68	7.60	7.66	7.72	0.854	0.862	0.888	0.907
3	7.56	7.46	7.52	7.56	0.816	0.815	0.840	0.846
4	7.36	7.23	7.31	7.36	0.752	0.742	0.771	0.781
5	7.21	7.07	7.17	7.25	0.705	0.691	0.722	0.739

	CASE 3.10 - Figure 21							
	speed deficit				**power deficit ratio**			
row	*dw=2o*	*dw=10o*	*dw=20o*	*dw=30o*	*dw=2o*	*dw=10o*	*dw=20o*	*dw=30o*

1	9.92	9.89	9.99	9.98	1.000	1.000	1.000	1.000
2	9.16	9.18	9.49	9.55	0.786	0.802	0.863	0.878
3	9.05	8.94	9.27	9.30	0.758	0.739	0.803	0.812
4	8.83	8.67	8.97	8.99	0.707	0.677	0.726	0.732
5	8.56	8.49	8.72	8.74	0.642	0.634	0.668	0.673